

Microstructure of Flash Processed Steel Characterized by Electron Backscatter
Diffraction

Chun-Hsien Wu

Thesis submitted to the faculty of the Virginia Polytechnic Institute and
State University in partial fulfillment of the requirements for the degree of

Master of Science In
Materials Science and Engineering

William T. Reynolds

Kathy Lu

Alex O. Aning

December, 7th 2009

Blacksburg, Virginia

Keywords: EBSD, OIM, misorientation, grain size, flash processing

Microstructure of Flash Processed Steel Characterized by Electron Backscatter Diffraction

Chun-Hsien Wu

Abstract

Flash processing is a new heat treatment process being developed to produce steel with relatively high strength and ductility. It involves rapidly heating steel sheet or strip to a temperature in the austenite range and quenching; the entire thermal cycle takes place within 15 seconds. The resulting microstructure is fine and difficult to resolve using standard metallographic techniques. In this investigation, electron backscatter diffraction was used to measure the grain size, grain orientations, and phase fractions in AISI 8620 samples flash processed to a series of different maximum temperatures. The combination of high strength with moderate ductility obtained by flash processing arises from a refined martensitic microstructure. The morphology of the microstructure depends upon the maximum processing temperature; a lower maximum temperature appears to produce a finer prior austenite grain size and an equiaxed martensite structure whereas a higher maximum processing temperature yields a more conventional lath martensite morphology.

Acknowledgements

I would like to thank my advisor, Dr. W.T. Reynolds Jr, for his instruction and the research support. Without his guidance and support I would not have learned the skills for doing the research and develop my own interest in materials science and engineering. I am really grateful for his advice during my time in the Virginia Tech and I feel lucky to be his student. He teaches me not only the knowledge of science but also the passion of being a scientist.

I would also like to thank SEM specialist, Stephen McCartney, for the SEM training, FIB specialist, John McIntosh, for experimental advice, and EBSD specialist, Richard McLaughlin, for the EBSD training. Moreover I wish to thank the NCFL at Virginia Tech for the providing research facilities and EBSD training.

Table of Contents

Abstract.....	ii
Acknowledgement.....	iii
Table of Contents.....	iv
List of Figures.....	v
List of Tables.....	vii
Chapter 1 Introduction.....	01
Chapter 2 Experimental.....	03
Chapter 3 Results and Discussion.....	08
3.1 Morphology.....	08
3.2 Grain Size.....	10
3.3 Volume Fraction.....	14
3.4 Phase Transformation Sequence.....	19
Chapter 4 Conclusion.....	20
References.....	21
Appendix A.....	23
Appendix B.....	28
Appendix C.....	31

List of Figures

Chapter 2 Experimental

Figure 2.1: (a) An inverse pole figure map of unprocessed AISI 8620 steel (annealed condition), (b) color map indicating crystallographic orientation of the surface normal, and (c) a typical electron backscattered diffraction pattern from one grain.....	06
--	----

Chapter 3 Results and Discussion

Figure 3.1: (a) An inverse pole figure map of AISI 8620 steel flash processed to a maximum temperature of 1066 C, and (b) a typical electron backscattered diffraction pattern from one grain.	09
--	----

Figure 3.2: (a) An inverse pole figure map of AISI 8620 steel flash processed to a maximum temperature of 1274 C and (b) a typical electron backscattered diffraction pattern from one grain.	10
---	----

Figure 3.3: Orientation imaging microscopy for morphology comparison.....	10
--	----

Figure 3.4: Grain size of flash processed samples as a function of maximum processing temperature.....	11
---	----

Figure 3.5: The distribution of misorientation angles for the annealed AISI 8620 steel with MacKenzie distribution (Random Theoretical misorientation distribution).....	12
---	----

Figure 3.6: The distribution of misorientation angles with Mackenize distribution (Random) for flash processed AISI 8620 steel processed at maximum processing temperatures (a) 1066 ° C, (b) 1093 ° C, (c) 1149 ° C, (d) 1260 ° C, (e) and 1274 ° C	14
Figure 3.7: The band slope distribution of flash processed AISI 8620 steel processed at maximum temperatures (a) 1066 ° C and (b) 1274 ° C.....	16
Figure 3.8: False ferrite grains in orientation image of flash processed AISI 8620 steel processed at (a) 1066 ° C and (b) 1274 ° C.....	18

Appendix B SEM Setup

Figure B.1: Drifting of Orientation Imaging Microscopy.....	29
--	----

List of Tables

Chapter 3 Results and Discussion

Table 3.1: Volume fraction of phases of flash processed AISI 8620 steel processed at different maximum temperatures.....	15
Table 3.2: Average band slopes of annealed (unprocessed) AISI 8620 steel and flash processed AISI 8620 steel.....	17

Appendix A EBSD Sample Preparation Procedure

Table A1: Sample Preparation Procedure.....	27
--	----

Chapter 1

Introduction

Crash safety and efficient fuel use make it desirable to develop stronger steels for automotive applications. At the same time, these steels must have sufficient ductility to allow them to be formed into complex shapes. Advanced high-strength steels [1] with yield strengths greater than 300 MPa and tensile strengths over 600MPa are being developed to fill this need. Sheet steels in the “Advanced High-Strength Steel” category include dual phase steels, transformation induced plasticity steels, complex phase steels and martensitic steels. “Flash processing” is a new heat treatment process which has the potential to produce high-strength microstructures through a relatively simple approach.

In flash processing [2,3], a thin section of steel is rapidly heated either by flame or by induction heating to temperatures in the range of 1000 to 1200 ° C within about 3 seconds and then quenched in water; the whole thermal cycle is accomplished within a period of 15 seconds. The flash processing technique has been shown to produce high-strength microstructures with moderate ductility in a variety of steel alloys [2, 3, 4]. An earlier study [2] reported the microstructure of a flash processed steel contains a mixture of carbides, bainite, and martensite. The present study was undertaken to explore the extent of austenite formation during flash processing and investigate the effect of the maximum flash processing

Chapter 1. Introduction

temperature on the microstructure.

Chapter 2

Experimental

The sample for this study is AISI 8620 steel 1.5mm in thickness (nominal composition in weight percent: 0.18-0.23 C, 0.70-0.90 Mn, 0.15-0.30 Si, 0.40-0.60 Cr, 0.40-0.70 Ni, 0.15-0.25 Mo). Five different flash processing conditions were considered: flame heating to a maximum temperature of 1066 ° C, 1093 ° C, 1149 ° C, 1260 ° C, and 1274 ° C, respectively, followed by a water quench. The effect of maximum processing temperature is investigated by characterizing the microstructure of these samples. The processing time for each of the flash processed samples above is the same, so the maximum temperature reached by the sample is the main variable influencing the microstructure of the flash processed samples.

All the flash processed samples had very fine microstructures that were difficult to resolve with optical microscopy, and while TEM has sufficient resolution to reveal some aspects of the microstructure, the limited volume of a TEM foil complicates interpretation of the overall microstructure without observing many foils. To avoid these shortcomings, orientation imaging with electron backscatter diffraction (EBSD) was used; it combines fairly high spatial resolution (20nm) with large sampling areas [5].

Electron Backscattered Diffraction arises from a region of a sample within roughly 50nm of its surface [6], and the sample-detector geometry requires a very flat

Chapter 2. Experimental

surface finish. For these reasons, samples for EBSD analysis must be very flat and free of polishing-induced surface damage or surface contamination. Sample mounting and polishing procedures were adjusted to give reproducible results on flash processed samples. A thermosetting epoxy mounting material was used for good sample edge retention, and sample mounts were masked with silver paint to ground the samples during analysis in the SEM. Good EBSD patterns were obtained with the rolling plane of the steel sheet oriented parallel to the mounting surface; flash processed samples whose rolling plane was perpendicular to the mounting plane (transverse sections) produced only occasional EBSD patterns of comparatively poor clarity.

Sample preparation consisted of successive grinding with 180, 240, 320, 600, 1200 grit SiC abrasive papers. Polishing was carried out with 5, 2.5, and 1 micron diamond paste on a non-woven textile/plastic polishing cloth, then 0.5 micron diamond paste on a canvas-backed rayon cloth, followed by a 20 minute polish with 0.05 micron alumina on a low-nap synthetic velvet cloth. The final step was a chemical/mechanical polish using 0.05 micron colloidal silica on a polyurethane low-nap cloth with a vibratory polisher. After each of the six polishing steps, samples were rinsed with water, cleaned ultrasonically in water for 5 minutes, and rinsed again with water. Detailed sample preparation procedures are listed in the Appendix A. Electron backscatter diffraction was carried out with an Oxford HKL Channel 5 system on a field emission LEO 1550 SEM. Details of the SEM setup are listed in Appendix B and the EBSD setup is listed in Appendix C.

Efficient EBSD mapping is sensitive to a number of microscope operating conditions and software settings. The best microscope parameters for the flash processed samples were a 12mm working distance, 18kV accelerating voltage, and a 120 micron condenser aperture. Software settings for collecting and analyzing EBSD patterns must be adjusted to provide a balance between indexing accuracy and analysis speed. The flash processed samples present a challenging combination of a fine microstructure and a significant amount of plastic strain.

Chapter 2. Experimental

To obtain sufficient sensitivity without giving up too much resolution, the EBSD detector was operated with 4x4 binning. Diffraction patterns were indexed using 5 or 6 reflecting planes, and only patterns with a mean angular deviation of less than 1.3 (from the expected pattern) were accepted. These settings indexed 70–90% of the patterns from flash processed samples and 98% of the patterns from annealed AISI 8620.

To establish the electron beam step size used in orientation mapping, it is necessary to have a reasonable estimate of the size of regions with a common orientation. To have an accuracy of 10% in grain size measurement it is necessary to index at least 5 pixels per grain, and for an accuracy of 5%, a minimum of 8 pixels per grain are required [7]. The linear intercept method applied to an EBSD line scan with a small step size was used to evaluate the approximate grain size. A step size of about one tenth of the average grain size is recommended for mapping [8], so a step size between 0.1 and 0.2 microns was used for mapping the flash processed samples. A noise reduction algorithm was employed over three successive frames to decrease the (small) number of incorrectly indexed points in each map.

Orientation imaging microscopy was conducted for both annealed and flash processed AISI 8620 steel. For the annealed condition, a suitable pattern quality for mapping in a reasonable time (about 30 minutes) was obtained using 8x8 binning and a 1um step size. Figure 2.1 (a) is an inverse pole figure map of annealed AISI 8620 steel. Each color represents the crystallographic direction of the normal to the sample surface; the correspondence between color and orientation is given by the stereographic triangle in Figure 2.1 (b). The black boundaries are high-angle boundaries arbitrarily defined as boundaries with a misorientation angle greater than 15 degrees. The infrequent red boundaries are low-angle boundaries with misorientation angles between 5 and 15 degrees. The unprocessed AISI 8620 steel microstructure has coarse, strain-free equiaxed grains.

Chapter 2. Experimental

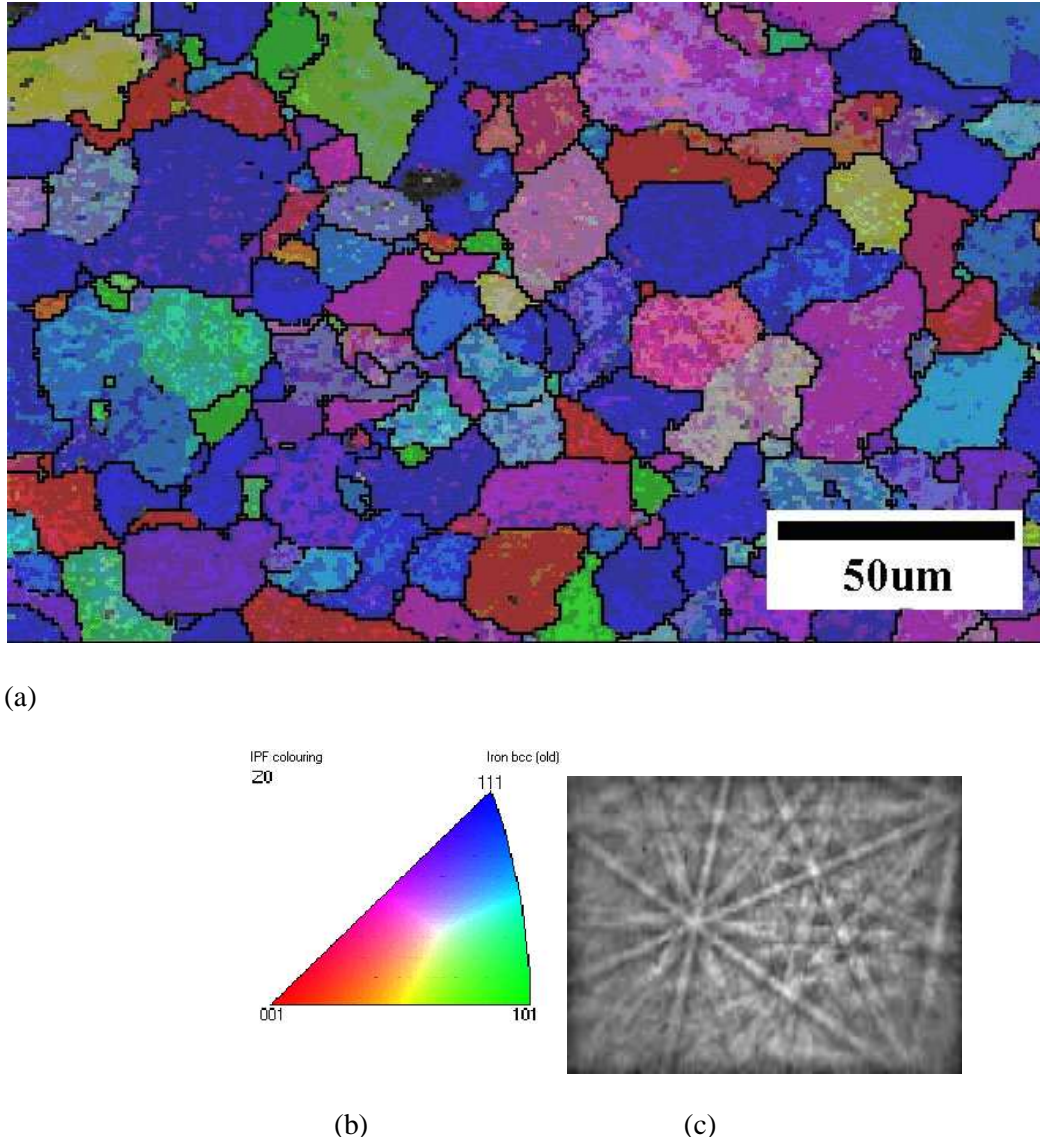


Figure 2.1: (a) An inverse pole figure map of unprocessed AISI 8620 steel (annealed condition), (b) color map indicating crystallographic orientation of the surface normal, and (c) a typical electron backscattered diffraction pattern from one grain.

The quality of electron backscatter patterns from flash processed steel is poorer than those from annealed samples, so 4x4 binning was adopted to increase the pattern quality and the step size was decreased to 0.2 μm to resolve the finer microstructure of flash processed samples. These combinations increased the data acquisition time to about 5 hours for a single

Chapter 2. Experimental

map for flash processed samples. Although all the flash processed conditions were analyzed with EBSD, the largest orientation maps were done for the lowest maximum processing temperature (1066°C) and highest maximum processing temperature (1274°C). A smaller condenser aperture (60um) is used for mapping the flash processed AISI 8620 steel processed at 1274°C to increase spatial resolution.

Chapter 3

Results and Discussion

3.1 Morphology

Figures 3.1 (a) and 3.2(a) are inverse pole figure maps of flash processed AISI 8620 steel with maximum processing temperatures of 1066°C and 1274°C , respectively. It is important to note that the subtle difference in lattice parameters of ferrite and martensite in this alloy are indistinguishable with EBSD, so these constituents appear as a single phase. Because plastic strains (higher dislocation densities) degrade the quality of EBSD patterns, it can be possible to distinguish between ferrite and martensite when there are significant differences in their respective dislocation densities [9,10]. This approach was useful for comparing the annealed sample with flash processed samples, but was ambiguous for differentiating the simultaneous presence of ferrite and martensite in flash processed samples.

The greater density of low-angle boundaries in Figures 3.1(a) and 3.2(a) suggests some dynamic recovery may have taken place during flash processing. Comparing the EBSD pattern of the annealed sample (Figure 2.1(c)) to the patterns of flash processed samples (Figure 3.1(b) and Figure 3.2(b)) shows the pattern quality of flash processed samples is poorer than the pattern quality from the annealed condition. The grains in flash processed appear considerably smaller than those of the annealed

Chapter 3.1 Morphology

sample in Figure 3.3, and they have greater variation in size. The features with a common orientation are roughly equiaxed in the sample flash processed at 1066° C , but they are larger and have a lath structure in the sample processed at 1274° C . These observations suggest the temperature excursion during flash processing is high enough (and long enough) to convert most, if not all, of the microstructure of this alloy to austenite, which subsequently converts to martensite upon quenching. However, for the sample processed to 1066° C (Figure 3.1 (a)) the relatively short time above the $\text{Ae}3$ (less than 3 seconds) may not be sufficient to produce a uniform distribution of austenite grains, and consequently, there is a large variation in the final martensite grain sizes. This prior austenite grains in the sample processed to 1274° C are evidently much larger, because the units of common orientation in Figure 3.2 (a) are larger than the grains in Figure 3.1 (a) and they have a more classic martensite lath appearance.

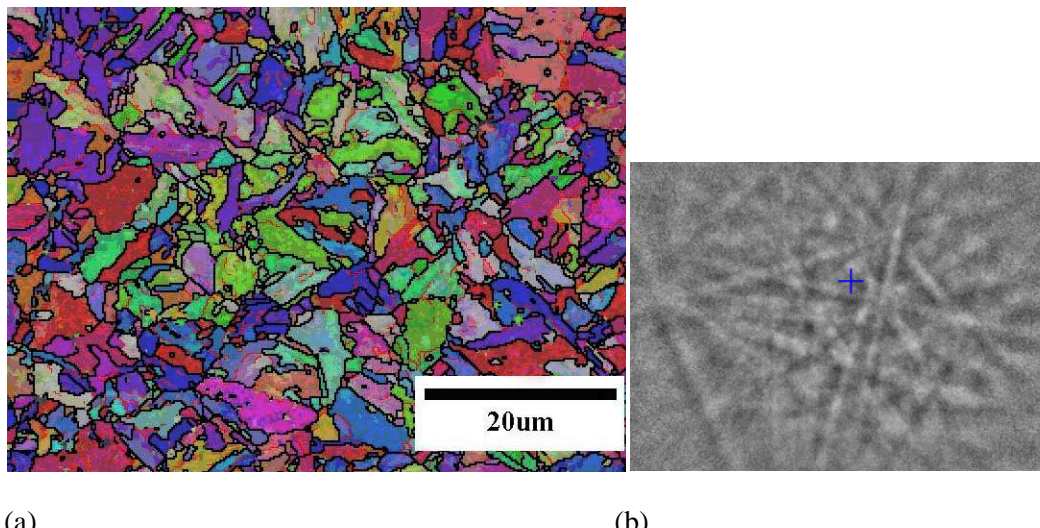
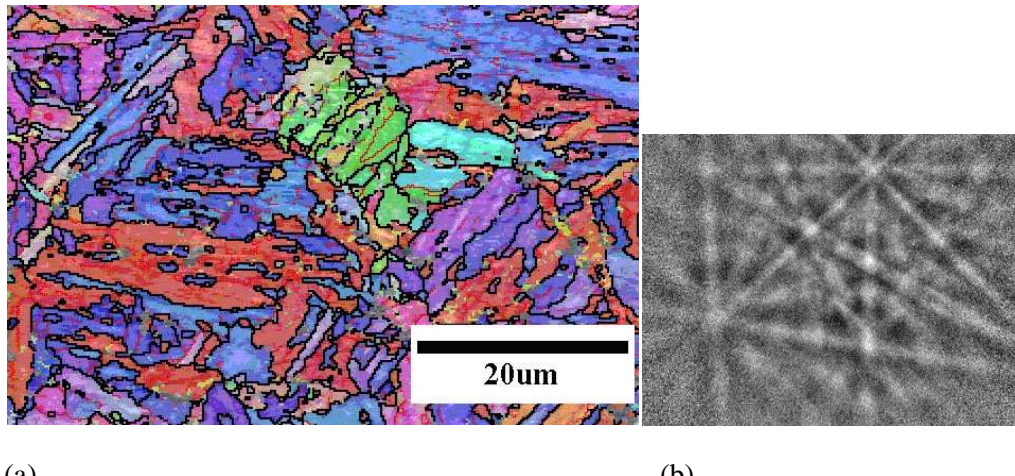


Figure 3.1: (a) An inverse pole figure map of AISI 8620 steel flash processed to a maximum temperature of 1066 C , and (b) a typical electron backscattered diffraction pattern from one grain.

Chapter 3.2 Grain Size



(a)

(b)

Figure 3.2: (a) An inverse pole figure map of AISI 8620 steel flash processed to a maximum temperature of 1274 C and (b) a typical electron backscattered diffraction pattern from one grain.

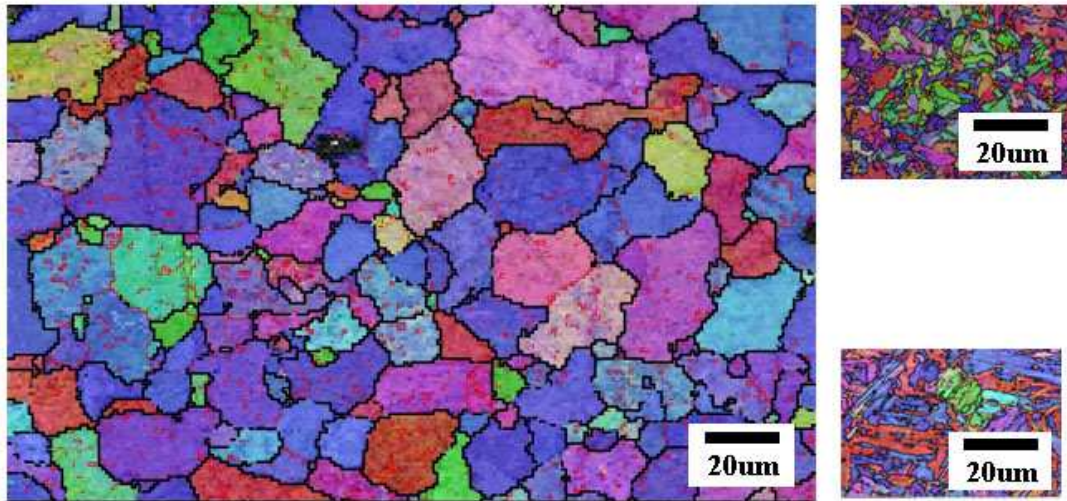


Figure 3.3: Orientation imaging microscopy for morphology comparison

3.2 Grain size

The linear intercept method [7] was used to measure the grain size from the orientation maps. Ten sampling lines were placed horizontally on each map with the

Chapter 3.2 Grain Size

lines distributed uniformly in the vertical direction. A minimum grain size threshold of five times the step size was used to prevent spurious contributions from indexing artifacts. The grain sizes measured this way have an accuracy of 10%. The average grain size is 13.1 microns in the annealed sample shown in figure 2.1 (a).

For samples flash processed at intermediate temperatures, the grain size was estimated using EBSD line scans (which avoids the lengthy microscope times needed to obtain orientation maps over large sample areas). The step size of the line scans was 0.1 microns and there were 10 lines for each flash processed temperature. Grains were measured along a total distance of 500 microns for each sample. A threshold minimum grain size of 0.8 microns was used for the line scan method. The accuracy of these grain size measurements is estimated to be 5%. The average grain sizes of flash processed samples are shown in Figure 3.4 as a function of the maximum processing temperature.

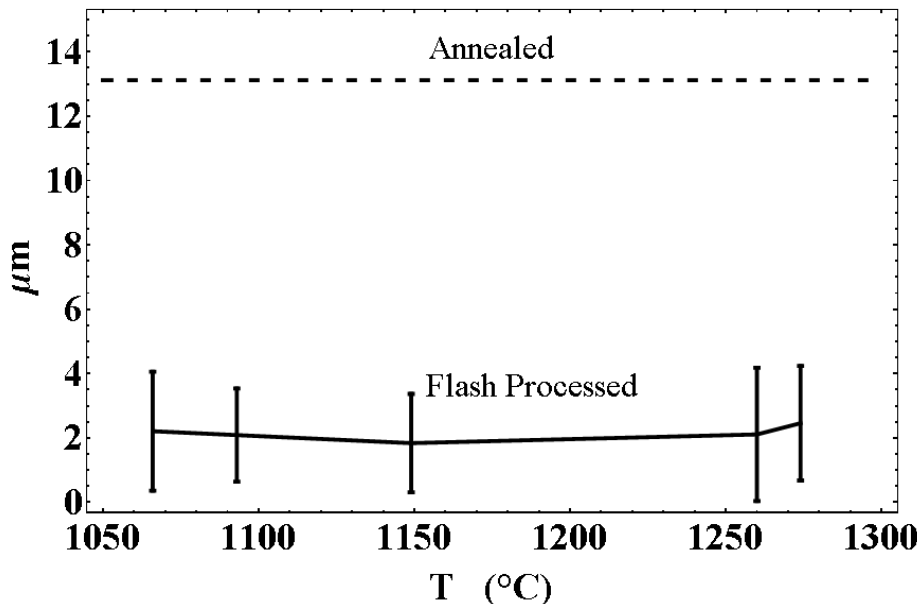


Figure 3.4: Grain size of flash processed samples as a function of maximum processing temperature.

Flash processing decreases the average grain size by a factor of 6.5 (from 13 microns to

Chapter 3.2 Grain Size

2 microns). Given the short thermal cycle, it seems unlikely this could happen without nearly complete austenitization during flash processing.

The distribution of correlated misorientation angles between grains was determined using the EBSD software. The correlated misorientation shows the misorientation between neighboring grains; Figure 3.5 is a representative example from the annealed AISI 8620 sample. The relatively high frequencies of low misorientations in Figure 3.5 come from low-angle boundaries. If the low angle misorientations ($< 15^\circ$) are excluded, the misorientation distribution is similar to the MacKenzie distribution (solid line) calculated for randomly oriented grains [13]. Thus, no discernable texture or trend was observed in the distribution of grain misorientations from the annealed sample.

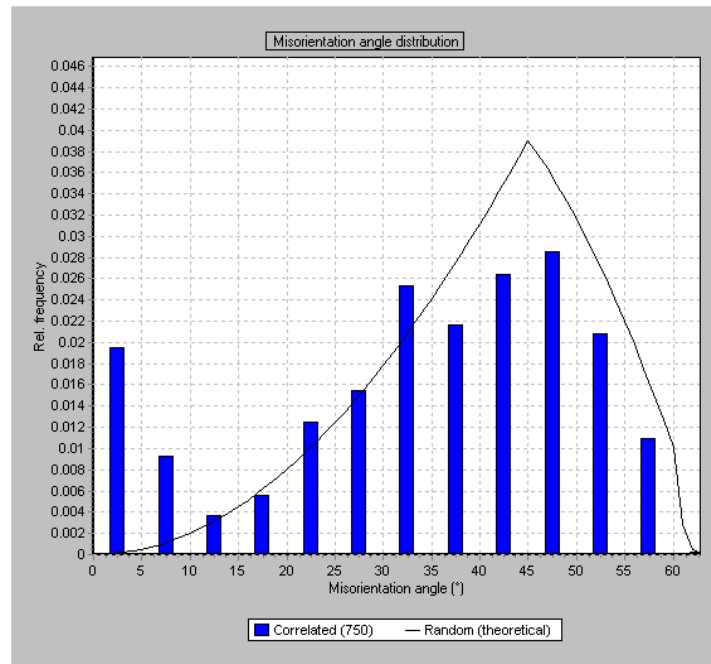
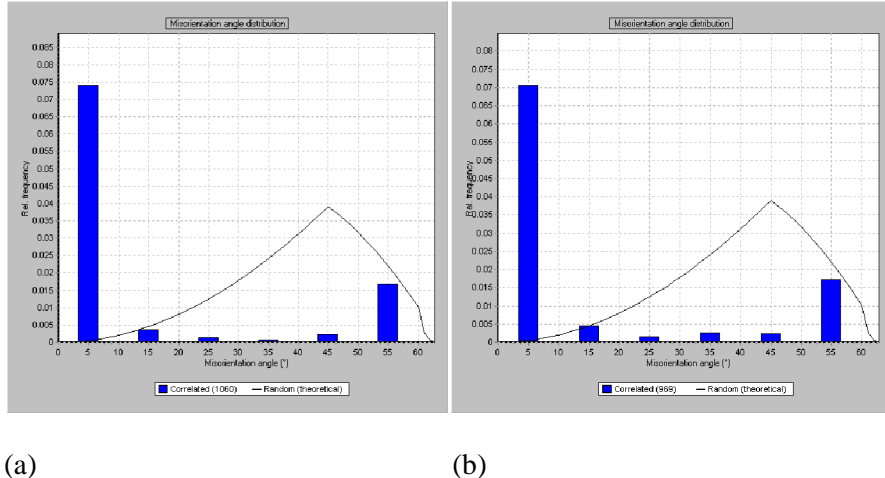


Figure 3.5: The distribution of misorientation angles for the annealed AISI 8620 steel with MacKenzie distribution (Random Theoretical misorientation distribution)

Figure 3.6 (a) to (e) are representative histograms of the misorientation distribution of the flash processed samples. The misorientation distribution data from flash processed

Chapter 3.2 Grain Size

samples were collected from at least 3 areas on samples from each of the different maximum processing temperatures. Unlike the misorientation distribution from annealed ferrite (Figure 3.5), the misorientation angles in flash processed samples have two distinct peaks: one at a misorientation angle of 5° and another at 55° . This trait is a signature of martensite grains. Typically, grain boundary misorientations in martensite cluster around low angle boundaries ($<15^\circ$) and high angle boundaries (50° to 63°) [11]. High angle misorientations are associated with martensite formed on opposite sides of prior austenite grain boundaries whereas low misorientations arise from the low-angle boundaries between martensite laths. All the flash processed samples share the same characteristic double peak in the misorientation distribution. Because this distribution is similar to that found in martensite [11], it appears likely that flash processing is producing a martensitic structure, and that implies the temperature excursion during flash processing fully austenitizes this particular steel.



Chapter 3.3 Volume Fraction

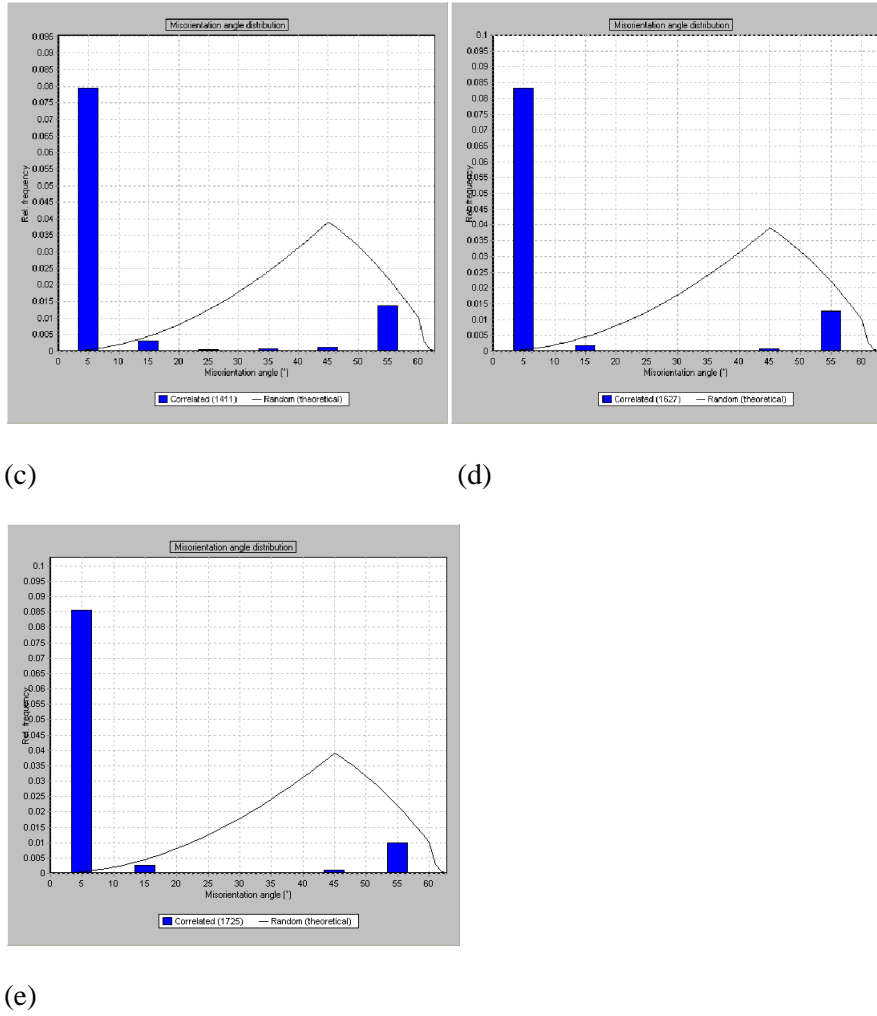


Figure 3.6: The distribution of misorientation angles with MacKenzie distribution (Random Theoretical misorientation distribution) for flash processed AISI 8620 steel processed at maximum processing temperatures (a) 1066 ° C, (b) 1093 ° C, (c) 1149 ° C, (d) 1260 ° C, (e) and 1274 ° C

3.3 Volume Fraction

The volume fractions of bcc phase (ferrite and martensite), of fcc phase (austenite), and of cementite in flash processed samples were measured with a point counting method [14] using indexed EBSD patterns to identify the phases at each point. For each processing temperature, a total of more than 800 points were sampled for point counting. The resulting volume fractions of the phases are summarized in the Table 3.1. The standard deviation of the

Chapter 3.3 Volume Fraction

volume fraction determination was about 0.5% for retained austenite and 0.75%-1% for cementite based on relative amounts of these phases and the number of points used to calculate the volume fractions [14].

The results in Table 3.1 were similar to phase fractions calculated from the large data sets used to generate the orientation maps of Figures 3.1 (a) and 3.2 (a). The cementite volume fraction is slightly overestimated in the point counting approach, presumably because the lower symmetry of cementite produces a few false positive identifications, and these cannot be eliminated from the point-count data using noise-reduction error checking as is done in two-dimension mapping routines. The cementite volume fraction in mapped samples was 1-2% with no significant difference among the different flash processing temperatures. The volume fraction of cementite seems to increase with maximum flash processing temperature and the volume fraction of retained austenite seems to decrease with maximum flash processing temperature; however, these trends may not be reliable because the error in the point counting method is similar in magnitude to these trends.

Maximum Flash Processing Temperature	FCC (%)	BCC (%)	Fe3C (%)	Total points
1066 ° C	1.95	93.67	4.38	821
1093 ° C	1.89	93.96	4.14	845
1149 ° C	3.23	90.56	6.21	837
1260 ° C	1.90	92.39	5.71	841
1274 ° C	1.66	91.56	6.78	723

Table 3.1: Volume fraction of phases of flash processed AISI 8620 steel processed at different maximum temperatures

Chapter 3.3 Volume Fraction

As noted previously, the quality of electron backscatter patterns is a measure of plastic strain [10]. When ferrite and martesite have significantly different dislocation densities, EBSD pattern quality (also called band slope) can then be used to distinguish between these two constituents [9,15]. The distribution of the band slope in the samples flash processed at 1066 ° C and 1274 ° C are shown in Figure 3.7 (a) and (b). In both samples, the band slopes appear to form a single, broad, normal distribution. There are no obvious breaks or features that might suggest low strain (ferrite) and high strain (martensite) constituents are both present in the samples at the same time [9].

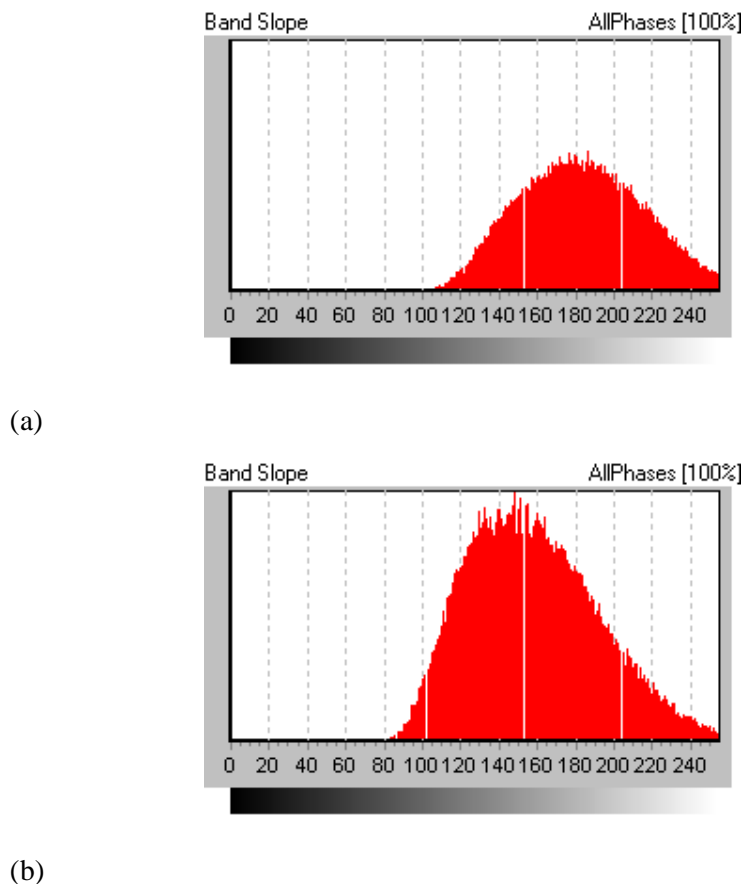


Figure 3.7: The band slope distribution of flash processed AISI 8620 steel processed at maximum temperatures (a) 1066 ° C and (b) 1274 ° C

The average band slopes of annealed (unprocessed) AISI 8620 steel and flash

Chapter 3.3 Volume Fraction

processed AISI 8620 steel are listed in the Table 3.2 (normalized to maximum value of 1).

The average band slope decreases dramatically after flash processing, as one would expect if flash processing replaces annealed ferrite with martensite. The higher maximum processing temperature decreases the band slope slightly more than the lower maximum processing temperature.

Samples Type	Average Band Slope
Annealed ferrite	0.98
Flash Processed, 1274 ° C	0.73
Flash Processed, 1066 ° C	0.75

Table 3.2: Average band slopes of annealed (unprocessed) AISI 8620 steel and flash processed AISI 8620 steel

The maximum band slope value is 255 and the average band slope of annealed AISI 8620 steels is 249.4. If a threshold of 240 is used to try to locate ferrite in orientation maps from flash processed samples, the results shown in the Figure 3.8(a) and (b) are obtained. The white background represents regions with average band slopes below the 240 threshold, and the color clusters represent possible ferrite grains. Possible ferrite grains are those grains in which 50% or more of the pixels have a band slope larger than the 240 threshold. The estimated volume fraction of ferrite using this criterion is 1.4% for the sample flash processed at 1066 ° C and only 0.2% for the sample flash processed at 1274 ° C. Given these small volume fractions, the extremely small sizes of the particles in Figures 3.8 (a) and (b), and noting that they do not have a recognizable ferrite morphology, it seems appropriate to conclude these regions are probably strain-free regions of martensite rather than ferrite. Thus,

Chapter 3.3 Volume Fraction

the band slope characteristics of the EBSD patterns also suggest the flash processed AISI 8620 steel is fully martensitic.

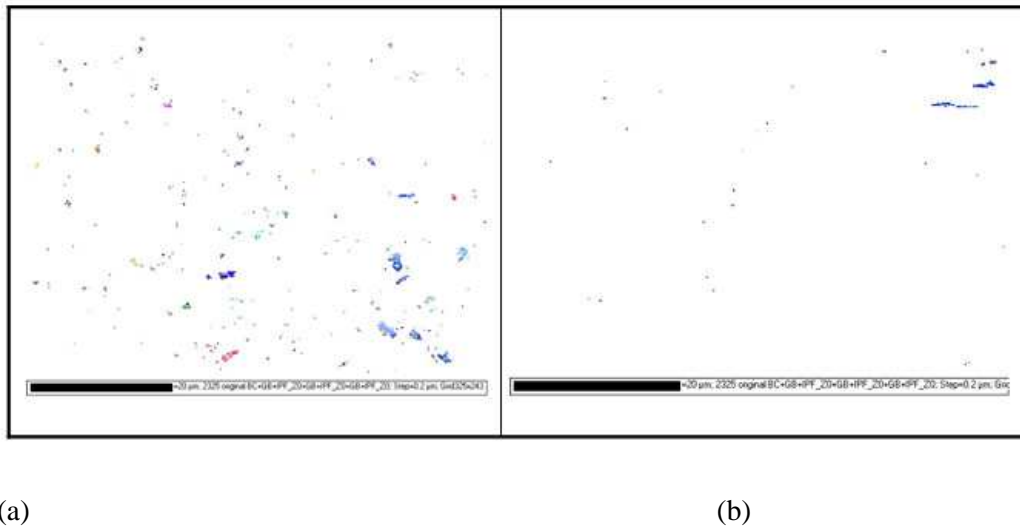


Figure 3.8:

False ferrite grains in orientation image of flash processed AISI 8620 steel processed at (a) 1066 ° C and (b) 1274 ° C.

Taken together, the grain morphology of the flash processed steel, particularly the lath structure at higher maximum processing temperatures, the bimodal misorientation distribution similar to that found in martensitic steels, the single band slope distributions, and the low band slope found in flash processed samples all strongly indicate the flash processing conditions studied here austenitized AISI 8620 and produced a fully martensitic structure upon quenching. The fact that a recent study [16] showed the tensile strength and yield strength of flash processed AISI 8620 steel are close to those of martensitic steel is consistent with this view.

3.4 Phase Transformation Sequence

The thermal cycle of flash processing includes rapid heating to an austenitization temperature and water quenching. The maximum flash processing temperatures of 1066 ° C, 1093 ° C, 1149 ° C, 1260 ° C, or 1274 ° C studied in this paper are all above the Ae3 estimated from the phase diagram so at least some transformation of ferrite to austenite is expected in the flash processing. As the microstructure in Figure 3.3 shows, the originally annealed ferrite is entirely replaced during flash processing. Although some of the ferrite and cementite in the original annealed microstructure could conceivably be retained during flash processing's short excursion to high temperature, the presence of a misorientation distribution characteristic of martensite and the absence of any indicators of ferrite in the band slope distributions indicate the ferrite is completely converted to austenite. A recent study of this steel [2] included TEM observations that suggested carbides may not be fully dissolved in austenite during flash processing. The carbide detected with EBSD in the current study is consistent with this finding, but the low volume fraction made it difficult to quantify the amount of undissolved carbide.

Chapter 4

Conclusions

The microstructure of the annealed AISI 8620 steel is changed dramatically by flash processing; the average grain size drops from 13 microns to 2 microns. Over 90% of the flash processed steel microstructure is a body-centered cubic phase. Retained austenite is less than 3% and cementite is less than 6% of the microstructure. The relative fractions of martensite and ferrite that make up the body-centered phase cannot be determined directly. However, the average band slope, misorientation distribution, and morphology of flash processed AISI 8620 steel strongly suggests there is very little, if any, ferrite in the microstructure and the microstructure is essentially fully martensitic.

The microstructure of the flash processed steel changes with the maximum processing temperature. Orientation imaging reveals martensite grains are fine and equiaxed after processing at the lower maximum temperature (1066° C). Larger, more conventional martensite laths are produced at the higher maximum processing temperature (1274° C). The higher processing temperature yields larger prior austenite grains that evidently allow martensite laths to form during quenching; the lower processing temperature produces smaller prior austenite grains that may be too small for conventional laths to develop.

References

- [1] R. Kuziak, R. Kawalla, and S. Waengler: Archives of Civil and Mechanical Engineering, 2008, Vol. VIII (No.2), pp. 103-117
- [2] T. Lolla, G. Cola, B. Narayanan, B. Alexandrov, and S.S. Babu: Materials Science and Technology, 2009, Vol. 000 (No. 000), pp. 1-13
- [3] G. Cola: ISIJ, 2007, pp. 186-190
- [4] G. Cola: Bainite Steel Company, Michigan, unpublished research, 2009
- [5] F.J. Humphreys: Journal of Materials Science, 2001, Vol. 36, pp. 3833-3854
- [6] M. M. Nowell, R. A. Witt, and B. True: Microsc Microanal, 2005, Vol. 11(Suppl. 2), pp. 504-505
- [7] F.J. Humphreys: Journal of Materials Science, 2001, Vol. 36, pp. 3833-3854
- [8] V. Randle: Materials Characterization, 2009, Vol. 60, pp. 913-922
- [9] A.W. Wilson, J.D. Madison, and G. Spanos: Scripta Materialia, 2001, Vol. 45, pp. 1335-1340
- [10] W. Zhou, Z. L. Wang: Scanning Microscopy for Nanotechnology Techniques and Applications, 1st ed., Springer, New York, NY, 2006, pp. 41-75
- [11] L. Ryde: Materials Science and Technology, 2006, Vol. 22 (No.11), pp. 1297-1306
- [12] A.P. Sutton, and R.W. Balluffi: Interface in Crystalline Materials, 1st ed. , Oxford Science, Oxford, UK , 1995
- [13] J.K. Mason, and C.A. Schuh: Acta Materialia, 2009, Vol. 57, pp. 4186-4197
- [14] T. Gladman, and J.H. Woodhead: Journal of the Iron and Steel Institute, 1996, Vol.194, pp. 189-193

References

- [15] J. Wu, P. J. Wray, C. I. Garcia, M. Hua and A. J. Deardo: ISIJ International, 2005, Vol. 45 (No.2), pp. 254-262
- [16] J. Zrnik, I. Mamuzic, and S. V. Dobatkin: METABK, 2006, Vol. 45(4), pp. 323-331

Appendix A

EBSD sample preparation procedure

EBSD requires very smooth surface compared with the surface for the SEM because the electron backscatter pattern (EBSP) is basically formed by the backscattered electron within 10~50nm of the depth of the surface and the EBSP is typically relatively weak to the background noise. Usually the pattern signal is only 5% on the top of the forward scattered background. Therefore if the surface roughness exceeds the limitation of 50nm or there is any residual surface deformation the EBSP quality will be too poor to index. So a flat sample surface is desired and any contamination of the surface should be avoided; thus, a good sample preparation is critical.

EBSD sample preparation includes the following steps.

Sample cutting

Sample mounting

Grinding

Polishing

Etch-Polishing

Each of the steps must be processed carefully. First a good sample cutting is essential. A bad sample cutting will result in heat damaged surface or high deformation surface.

Appendix A

Second in addition to have a well polished surface a well edge protected sample mounting material should be chosen. Normally the conductive mounting material is chosen for metallurgy mounting in order to prevent the charging problem in the SEM; however, the flash processed samples are very surface sensitive because of the processing. The steel sheet is cooled from high temperature to low temperature rapidly and there is phase transformation inside the steel. Both of them will result in high strains within the samples. So the EBSP is poor naturally. So any slight contamination or residual deformation will affect the EBSP tremendously. The conductive mounting material with carbon filling has been used but it will result in a contamination layer of carbon on the surface and mounting materials with copper is tested but it is soft so it will cumulate diamond particles during the polishing process and result in scratches on the surface. Instead of conductive mounting materials, the non-conductive mounting material is adopted. The flash processed samples are mounted with the fine mounting powder (Epomet F, Buhler) which has superior edge protection and the copper tape has been used to eliminate the charging problem. Although the ideal mounting material has been decided, a desired grinding and polishing procedure needs to be determined.

Based on different hardness of materials, the sample preparation will be different. Hard materials usually take more time to remove the scratch surface than soft materials and different polishing cloth will also affect the polishing result. In order to develop a desired sample preparation procedure, three control samples (untreated AISI 8620, Ni alloy and W) have been mounted with flash processed AISI 8620 samples on the same mount. Untreated AISI 8620 has lower hardness than flash processed ones and Ni alloy has the similar hardness to flash processed ones and W has higher hardness. After the sample preparation by checking the secondary electron image on the SEM, the flatness of the sample surface can be examined. If the surface of the sample is not flat the procedure needs to be modified otherwise check the EBSP quality. If the quality of EBSP is very poor, a layer of contamination or deformation is

Appendix A

possible. Again the preparation procedure needs to be modified. For flash processed samples, there is a layer of colloidal silica on the surface so a clean pad is used to wipe the layer out. If the control sample has the EBSP but flash processed ones don't, a layer of contamination can be eliminated because the samples are on the same mount; then, it is deformation problem. Typically hard sample is hard to be deformed and soft sample is easier to be deformed. By comparing the pattern quality of control and flash processed samples the sample preparation procedure can be adjusted and an ideal sample preparation can be developed. The optimized sample preparation procedure is listed on the following Table A1.

Grinding		
Grinding Paper	Conditions	
180 Grit SiC paper	Grind until the surface becomes flat	
240 Grit SiC paper	Grind until the scratches in the same direction	
320 Grit SiC paper	Grind until the scratches in the same direction	
600 Grit SiC paper	Grind until the scratches in the same direction	
1200Grit SiC paper	Until the scratches in the same direction. Observe carefully with optical microscope.	
Polishing		
Polishing paste	Polishing cloth	Conditions
5um diamond paste	Kem Pad (Allied)	Manual polish the sample until the 5um scratches become random distributed. Rinse With water and clean with ultra sonic cleaner for 5mins and rise with water.
2.5um diamond paste	Kem Pad	Manual polish the sample until the 2.5um

Appendix A

	(Allied)	scratches become random distributed. Rinse With water and clean with ultra sonic cleaner for 5mins and rise with water.
1um diamond paste	Kem Pad (Allied)	Manual polish the sample until the 1um scratches become random distributed. Rinse With water and clean with ultra sonic cleaner for 5mins and rise with water.
0.5um diamond paste	Final B (Allied)	Manual polish the sample until the 0.5um scratches become random distributed and rinse with water and clean with ultra sonic cleaner for 5mins and rise with water.
0.05 alumina	Vel Cloth (Allied)	Manual polish for 20mins and rinse with water and clean with ultra sonic cleaner for 5mins and rise with water.
Etch- Polishing		
Polishing substance	Polishing Cloth & Instrumrnt	Condition
0.05 Colloidal Silica	ChemPal (Allied) with Vibration Polisher	Use the vibration polisher to polish the sample for 30min and rinse with water and clean with ultra sonic cleaner for 5mins and rise with water. Final step is to use the clean dry chem pal to wipe the surface of sample

Appendix A

	(Buhler)	to remove contamination layer.
--	----------	--------------------------------

Table A1: Sample Preparation Procedure

At the beginning, the surface of rolling direction of flash processed AISI 8620 steel is mounted perpendicular to the mount surface. After a series of polishing none of good EBSP of flash processed samples can be observed. However after the flash processed samples are remounted with the surface of rolling direction parallel to the mount surface, a good EBSP appears.

Before going to SEM, the sample must be grounded for sure otherwise as the times goes on the EBSD mapping will drift. Usually it takes an hour or several hours to acquire a single EBSD mapping so this simple step must be checked. Typically copper tape and silver paint are good choice for grounding.

Appendix B

SEM Setup

Before running any orientation mapping the charging problem must be eliminated for sure because drifting is a common problem in OIM mapping especially when the high resolution orientation mapping is conducted. Moreover if the data acquisition time is very long the drifting problem may increase with time also. Masking sample with silver paint is a good choice for grounding the sample. There is another problem must be aware. There is another problem must be aware. The stage must be stable at all times during the mapping otherwise the orientation map drifts too. The Figure A.1 below is a orientation map with drifting in the lower part of the image. In this case the sample is not stabilized on the sample holder so as times goes by the sample drops down for several microns and the lower part of the image is blurred. As a result, grounding and sample stabilization are significant before putting the sample into electron microscope.

Appendix B

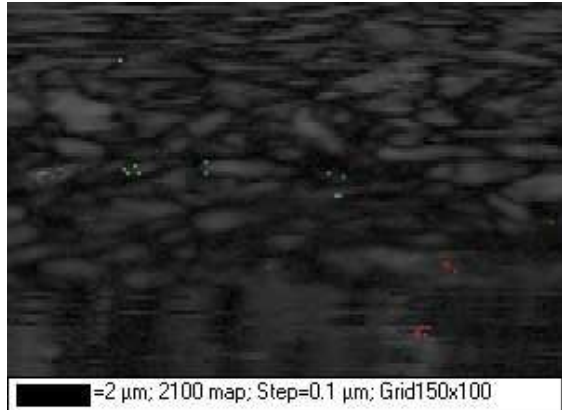


Figure B.1: Drifting of Orientation Imaging Microscopy

In order to have best electron backscatter diffraction quality, there are some parameters of scanning electron microscope needed to be adjusted. They include working distance, beam energy, dynamic focus, stigmation and aperture.

In consideration of working distance, higher working distance results in better depth of focus but lower working distance results in small probe size. Typically lower working distance is desirable because the spatial resolution of electron backscatter diffraction increases with smaller probe size. The beam energy affects the depth of penetration and distance of scattered electrons traveled. If the microstructure is fine, low beam energy is desirable because the noise from the nearby grains decreases but if the beam energy is too low the backscatter signal is too low to form a pattern; therefore, intermediate beam energy is desirable in the SEM setting. The dynamic focus is very important in the setting because the normal of the sample stage is tilted 70° from the electrons beam so it is easily out of focus in the direction perpendicular to the tilt axis; therefore, the dynamic focus must always be on during orientation mapping. Generally if the sample is not in focus the probe size gets larger and the resolution gets poor. When dynamic focus is off, The image quality of orientation imaging microscopy gets poor in the direction perpendicular to the tilt axis. In the other hand the stigmation is the similar issue. The stigmation must be adjusted to have secondary electron image in focus also. The last parameter is aperture. For high speed mapping the large

Appendix B

aperture is desired so there will be more electrons going through the aperture and the timing per frame reduces because the EBSD detector can detect more backscatter electrons but more electrons going through also means that there are more noises from the nearby grains so for high resolution mapping small aperture is recommended. However if the aperture is too small either the backscatter electrons are not enough to form distinguishable electron backscatter pattern or the time for frames integration is tremendous. As a result, intermediate aperture and beam energy is desirable.

Appendix C

EBSD Setup

The EBSD data acquisition system used in this experiment is HKL Channel 5 system (Oxford Instruments). Before running the orientation mapping, several recommended steps are listed below.

Imaging

Setting

Map setting

The HKL channel 5 system has the function to show both the secondary electron and back scatter electron image. Typically secondary electron image should be flat and no residual or blemish on the surface otherwise the sample preparation needs to be adjusted. Once the secondary electron image is checked; then the backscatter electron image needs be checked also. If the image is blurred, the sample preparation probably needs to be adjusted again because there might be heavy deformation inside the surface. After the backscatter electron image is clear, the dynamic focus and stigmation must be adjusted to have image in focus because the Kikuchi bands are generated by the backscatter electrons.

Appendix C

After the adjustment, a sharp electron backscatter diffraction pattern is anticipated. Once the imagining is ready, the calibration, timing per frame, number of frames for noise reduction, binning, background correction, number of bands detected, match units and mean angular deviation must adjusted to have best electron backscatter patterns.

First, the most important of all is the calibration of the EBSD system. In order to have accurate orientation imaging and reliable solutions the calibration must be processed before the orientation mapping. The goal for the calibration is to define the center of the electron backscatter pattern which is the interception point between the ray perpendiculars to the electron beam and tilt axis and phosphor screen. The pattern center has two variables. One is working distance; the other is the position of EBSD detector. In order to calibrate the HKL Channel 5 system a known orientation material is indexed by the system. Mostly the single crystal silicon wafer is used to calibrate the EBSD system. By indexing the wafer and refining the matching Kikuchi bands the pattern center is refined and well calibrated.

After the EBSD system is calibrated, the setting must be adjusted to have optimized electron backscatter pattern quality and acceptable data acquisition time. The primary parameter should be decided is the binning. The binning defines the area of the charge-coupled device camera to detect the electron backscatter pattern. For example 8x8 binning means that there are 64 pixels counted as one super pixel; therefore, the sensitivity will increase 64times but the resolution will be decrease 1/64 times. The more sensitive the camera is; the shorter timing per frame is; the shorter data acquisition time is but if there is heavy deformation on the sample surface 8x8 binning is not ideal because the pattern quality is relatively poor for indexing as a result 4x4 binning is more considerable or even 2x2 binning.

Before having a diffraction pattern, the background must be corrected. The background is collected by averaging the signal of raster scan on imaging area. After the background is collected the electron backscatter pattern of the point spot can be observed by dividing the

Appendix C

background signal. In addition to have optimized pattern quality the number of frames for background correction must be optimized. Besides the background correction there are two other parameters affecting the EBSP quality: timing per frame and number of frames for noise reduction. The timing per frame is the exposure time of the phosphor screen per frame and the number of frames for noise reduction is the number of frames averaging for electron backscatter pattern. If timing per frame is too long; then, the background will turn white and if it is too short; then, the background will turn black. Moreover the data acquisition time is proportion to the timing per frame multiplied by the number of frames for noise reduction. As a result, by optimizing these two parameters the reasonable data acquisition and pattern quality for indexing can be achieved.

After the electron backscatter pattern is reasonable for being indexed, the match units need to be selected. Match units can selected from the expected phases based on phase diagram. Followed by selecting the match units, the number of detected bands must be decided. It is the number of bands detected to match with the solution in the EBSD crystal data base. The higher the number of bands detected is the higher chance of accuracy the solution is. Normally 4 to 5 bands are used to index the phases.

The last parameter is mean angular deviation [8] which describes how well the actual electron backscatter pattern matches with simulated one. Usually mean angular deviation less than 1.3 is reasonable data; therefore, the minimum mean angular deviation is typically setup as 1.3 and the data acquisition system only stores the data of the MAD less than or equal to 1.3 .

If all the parameters are optimized manually check the indexing of the electron backscatter pattern and see whether the actual electron backscatter pattern matches up with the simulated one. Several points of indexing must be conducted to have confidence of indexing before mapping. After the indexing section is proper, the grain size needs to be estimated first. Proper step size and area are required to have accurate grain size

Appendix C

measurement. In addition to have an accuracy of 10% in grain size measurement at least 5 pixels per grain are required, and for an accuracy of 5%, a minimum of 8 pixels per grain are required. So running a single line scan to estimate the approximate grain size in smaller step size is recommended and use estimated grain size to decide the proper step size. A step size around one tenth of the averaged grain size is recommended for mapping. In order to statistical grain size measurement over the sample at least 200 grains are required within the map and each grain needs 5-10 pixels across to have accuracy. Therefore around 20000 pixels are required for a single map.